Available online at www.sciencedirect.com
SCIENCE DIRECT®
Computers and Chemical Engineering 27 (2003) 1473–1484
Computers & Chemical Engineering
www.elsevier.com/locate/compchemeng

Computationally efficient algorithms for modelling thermal degradation and spiking phenomena in polymeric materials

R.V.N. Melnik *

Faculty of Science and Engineering, Mads Clausen Institute, University of Southern Denmark, Grundvigs Alle 150, DK-6400 Sonderborg, Denmark

Received 9 March 2001; received in revised form 10 March 2003; accepted 10 March 2003

Abstract

In many areas of chemical engineering applications we have to deal with thermosetting polymer structures. One of the major processing techniques for producing such structures is the curing process. This process may be accompanied by undesirable thermal spiking phenomena during which the released energy may be trapped inside of the structure. In order to predict the onset of this phenomenon models that couple reaction kinetics and heat transfer are required. In this paper we propose an efficient algorithm for the solution of such coupled problems. The algorithm is based on the alternating-triangular methodology which is more efficient compared to ADI methodologies conventionally applied to similar problems. The algorithm is described in detail. The results for simulations of reaction kinetics are compared with those obtained in the literature from experimental measurements. A series of numerical experiments for the fully coupled system are also presented.

Keywords: Coupled problems; Polymer systems; Thermal degradation and spiking; Alternating-triangular method

1. Introduction

Many problems arising in chemical engineering applications are essentially coupled in a sense that they require to deal with the dynamics of two or more different processes and/or physical fields that are intrinsically connected and influence each other. In this paper we are interested in one such problem, namely in the modelling of curing dynamics of polymeric materials. These materials embrace the whole range of chemical engineering applications including applications of polymeric composites, elastomers, thermosets, thermoplastics, polymer colloids, coatings, films, copolymers, polymer blends, and polymeric biomaterials. The materials range substantially in terms of their processing techniques and the resulting properties. For example, thermosetting materials, in contrast to conventional thermoplastics, require more delicate techniques at the processing stage, but this is paid off by the fact that the resulting materials are more stable in terms of creeping and softening under higher temperature. As a result, thermoset composites have an increasing demand in such areas as the encapsulation of computer chips (to protect metallic layouts exposed to electrical current), communication industry, and biomedical applications to name just a few. In many such applications a better dimensional stability and higher thermal resistance are the key factors that determine a wide spread success of these materials (Flipsen et al., 1996). However, while producing thin polymeric thermoset composites is a well-established technological process, several inherently difficult problems exist in the production of thick composite structures. One of the most important among them is the thermal lag and spiking phenomena pronounced at the stage of curing. These phenomena may contribute substantially to the overall thermal degradation of the material at the stage of material applications. To predict the onset of thermal spiking is not an easy task, and in order to approach the solution of this task we need to apply models that couple the dynamics of heat transfer to chemical kinetics. Such models require efficient computational algorithms that would allow us to deal with steep gradients in the solutions and with nonlinearities of coupled dynamics. Recently, the im-

* Tel.: +45-6550-1681; fax: +45-6550-1660.
E-mail address: rmelnik@mci.sdu.dk (R.V.N. Melnik).

0098-1354/03/$ - see front matter
doi:10.1016/S0098-1354(03)00093-0

portance of coupled solution of models for heat transfer and chemical reaction models have been emphasised by several authors (e.g. Li, Sun, & Lee, 1999; Ding et al., 2000).

In this paper we propose a new approach for modelling coupled dynamics of chemical reaction and heat transfer in polymeric materials. The approach, based on the alternating-triangular methodology, is discussed here in the context of modelling thermal spiking phenomena in thick composite layers. The paper is organised as follows. In Section 2 we give a brief overview of the problem of thermal degradation and formulate the mathematical model we are dealing with in the subsequent sections. Section 3 is devoted to the description of the algorithm on which our computational code is based. Details of the implementation with ordered set of iterative parameters are also given in this section. In Section 4 we describe the results of our computational experiments demonstrating capabilities of the algorithm to reproduce experimentally available data on reaction kinetics for acrylic resins, and to predict the onset of thermal spiking in thick samples of these polymers.

2. Model formulation and governing equations

Thermal degradation of polymeric materials is a consequence of the fact that all organic macromolecules as well as low-molecular weight organic molecules are stable only below a certain limiting temperature, which is much lower compared to many inorganic materials. Since molecules are composed of atoms linked together by covalent bonds and the strength of these bonds is limited (dislocation energies of single bonds in the ground state are in the order of 140–420 kJ mol^{-1} at 25 °C), a high thermal sensitivity of organic substances can be explained at the molecular level because scissions of chemical bonds under the influence of heat are the results of overcoming bond dissociation energies. However, the methodologies based on the idea of tracing time-and-rate-dependent thermochemical (and viscomechanical) properties of polymers back to their origin at a molecular level that lead to the application of different molecular modelling techniques (see, for example, Melnik, Uhlherr, Hodgkin, & de Hoog, 2003; Tokarski et al., 1997 and references therein) are computationally very costly, and in their full implementations are typically impractical for routine engineering runs from a computational point of view. On the other hand, usual analytical methods might fail in detecting chemical changes in polymer systems induced by their degradation. Under these circumstances, the development of macroscopic mathematical models and numerical methods for their solution that incorporate a coupled effect of chemical kinetics and heat transfer allowing the prediction of such changes becomes an important and challenging task in chemical engineering (Covas, 1994).

In what follows, our major focus will be on the modelling of the phenomena associated with the curing process of thermoset resins, a key process in the manufacturing of these materials. It is an irreversible process which requires accounting for many different features in order to produce a high-quality rigid cross-linked molecular structure. Some such features will remain beyond the scope of the present paper. For example, the molecular weight dependency of the stress relaxation modulus is certainly an important factor to the understanding of viscous effects in polymer systems. Due to a high sensitivity of viscosity to temperature changes and in the end essentially non-Newtonian rheological properties of the (molten) polymer, it is also important to pay attention to the possibility of generation of high stresses which might contribute to material failures. We refer the reader interested in these issues to Mohan and Grentzer (1995), Adolf et al. (1998), Covas (1994), Li and Lee (1998) and Cristini, Macosko, and Jansseune (2002) for practical examples and mathematical models related to the associated problems. In this paper we concentrate on modelling thermochemical properties of thermosets that at a later stage can be effectively coupled to the modelling of such mechanical properties as stresses, and hence can lead to accurate prediction of shrinkage during thermoset curing.

Our further discussion is based on the fact that the behaviour and properties of polymeric materials are determined largely by processes of heat and mass transfer which, in their turn, depend strongly on the degradation reactions. In the general case, polymerisation kinetics in thermoset composites during the cure is a fairly complex process due to the fact that the cure kinetics is determined by relating cross-linking (connected in a complex manner with conversion) and the dynamics of heat generation response. In deriving a model for polymerisation kinetics we have (a) to take into account the diffusion effect in the models, (b) to couple the kinetic model with the energy balance equation, and (c) to account for the fact that depending on temperature conditions we can achieve usually only a partial resin cure (or conversion) due to quenching of the reaction (Mohan & Grentzer, 1995; Nzihou, Sharock, & Ricard, 1999). A computational code developed as a result of our analysis allows us to deal with a quite general model for the reaction kinetic with five degrees of freedom

$$\frac{dG}{dt} = \tilde{K} G^{\beta_1} (G_{\max} - G)^{\beta_2} (1 - G)^{\beta_3}, \tag{2.1}$$

where $\tilde{K}$ is a function of temperature determined as $\tilde{K} = \tilde{K}_0 \exp(-\varepsilon_A / RT)$, where ε_A is the activation energy, $\tilde{K}_0$

and R are given kinetic constants (pre-exponential and gas constants, respectively), and β_1, β_2, and β_3 are exponents determined through the experiment. Further, G is the cumulative conversion (extent of cure) at a given time t and $G_{\max}$ the maximum conversion at a given isothermal cure temperature. Note that the partial conversion is accounted for by the term containing β_2, and the conversion rate is zero if $G = G_{\max}$. This term could also be written as $(1-(G/G_{\max}))\beta_2$ with appropriate changes made to the pre-exponential coefficient $\tilde{K}$.

Our computational experiments reported in Section 4 deal with acrylic composites. It is known that model (2.1) provides a very good experimental fit for these materials (Maffezzoli & Terzi, 1998; Nzihou et al., 1998). To demonstrate this, we present both conversion and conversion rate for the acrylic resin modelled with Eq. (2.1) in a range of temperature conditions. Parametrisation of the model for the material of interest is as follows:

$$\tilde{K}_0 = 4.76 \times 10^9, \qquad T_A = 8207,$$
$$G_{\max} = 0.018T - 5.034, \qquad \beta_1 = 0.7, \qquad \beta_2 = 0.9, \quad (2.2)$$
$$\beta_3 = 1.$$

The results, obtained with models (2.1), (2.2), and that presented in Figs. 1 and 2, reproduce very well the dependencies obtained experimentally with differential calorimetric measurements (e.g. Nzihou et al., 1998, 1999).

The cure is one of the most critical processes in manufacturing thermoset composites. In order to model this process the chosen model for chemical kinetics should be coupled to a model for heat transfer. Before proceeding to the heat transfer part of our model we note that in many applications polymeric materials are used in the form of thin structural components. While there are well-established technological procedures for producing such structures, manufacturing thick polymeric components, important in many industries (Kim et al., 1995), is connected with several inherently difficult problems. From a physical point of view, we have to deal with large barriers during heat-up/cool-down of such materials due to their low thermal conductivities. What happens is that as soon as the interior of the future product heats up, the exothermic curing reaction starts by releasing energy which is often trapped in the interior. This phenomenon, known as thermal spiking, is often attributed to poor thermal conductivity. A basic consequence of this phenomenon is that the entrapped heat raises the temperature of the structure further,

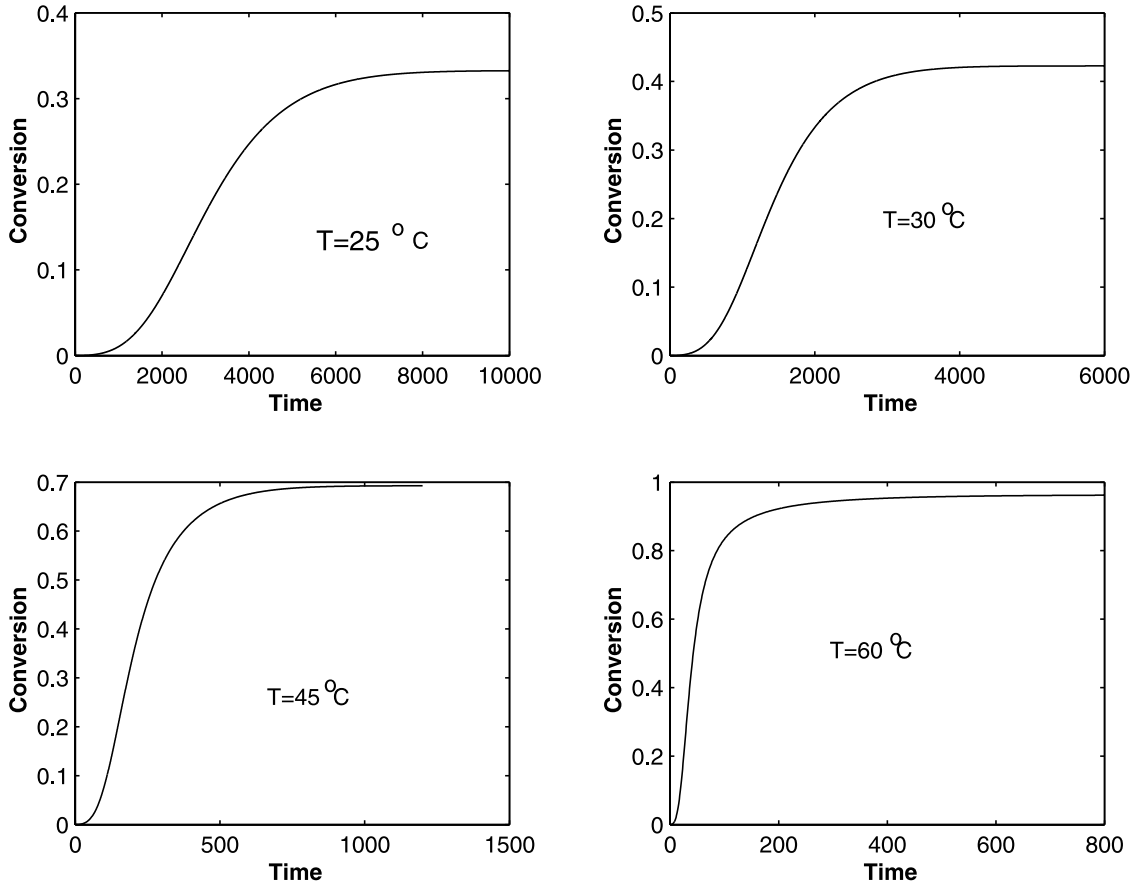

Fig. 1. Conversion for different temperatures.

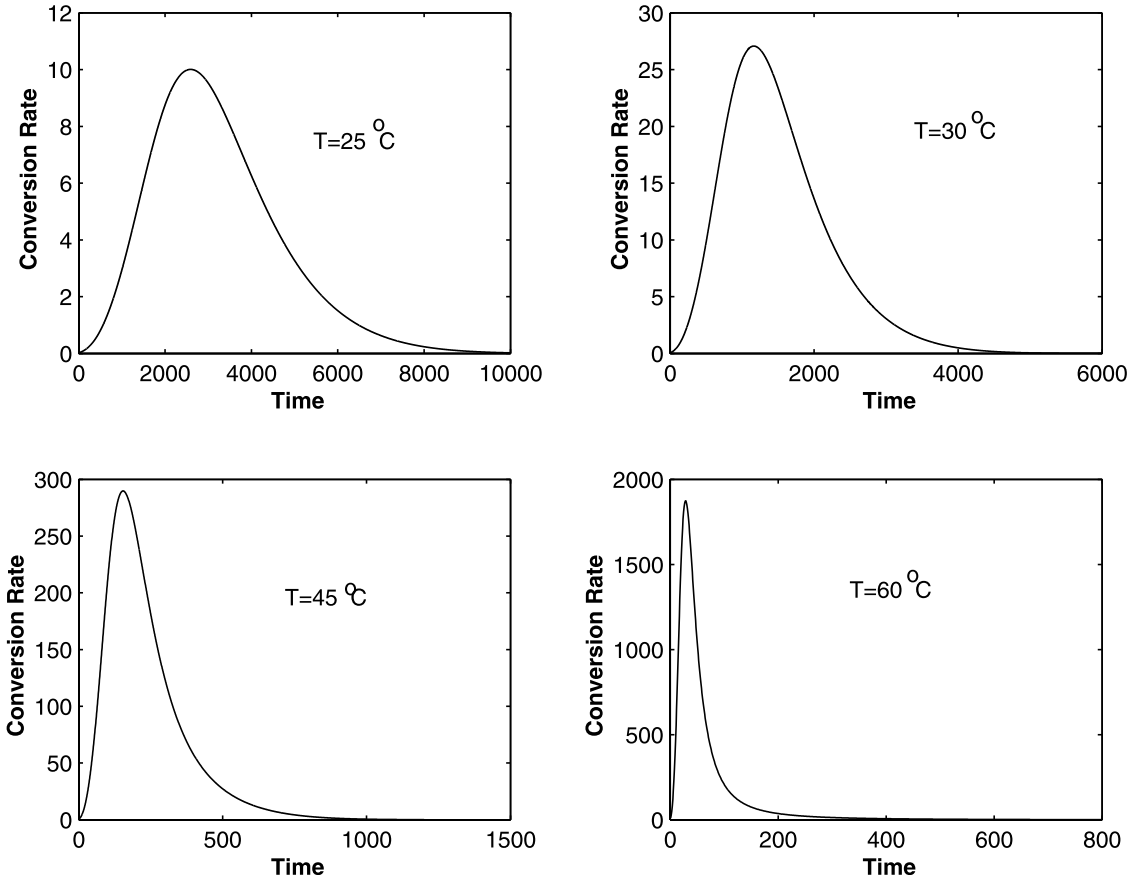

Fig. 2. Conversion rate for different temperatures.

stimulating faster curing and more rapid energy release, and leading to a possibility of instability of the process (Kim et al., 1995). In some cases, the onset of this phenomenon can be predicted with analytical tools (Buckmaster & Vedarajan, 1997), while in more complicated situations numerical simulations are required. Such simulations are based on the coupled dynamics of chemical kinetics and heat transfer. The model for the heat transfer in the polymeric material of cylindrical shape can be written as follows:

$$r\rho_p C_p \frac{\partial T}{\partial t} = \frac{\partial}{\partial r}\left(rk_p \frac{\partial T}{\partial r}\right) + \frac{\partial}{\partial z}\left(rk_p \frac{\partial T}{\partial z}\right) + f^0, \qquad (2.3)$$

where ρ_p is the density, C_p the heat capacity, and k_p the coefficient of thermal conductivity of the polymeric material under consideration. The right hand side of Eq. (2.3) should account for the total heat of reaction of the thermoset material. It is a nonlinear function of T, and is dependent on the reaction rate, and realises the coupling between the heat transfer and chemical reaction intrinsic to the process of curing. Basically, we need to establish an equation that connects the heat generation, dH/dt, and the reaction (conversion) rates, dG/dt. By using the standard definition of the reaction rate (e.g. Torre, Maffezzoli, & Nicolais, 1995), we assume the linear dependency between these two quantities (e.g.

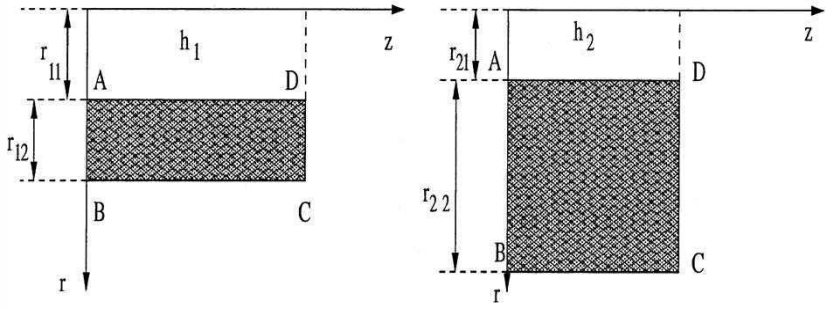

Fig. 3. Computational domains for thin and thick polymer layers.

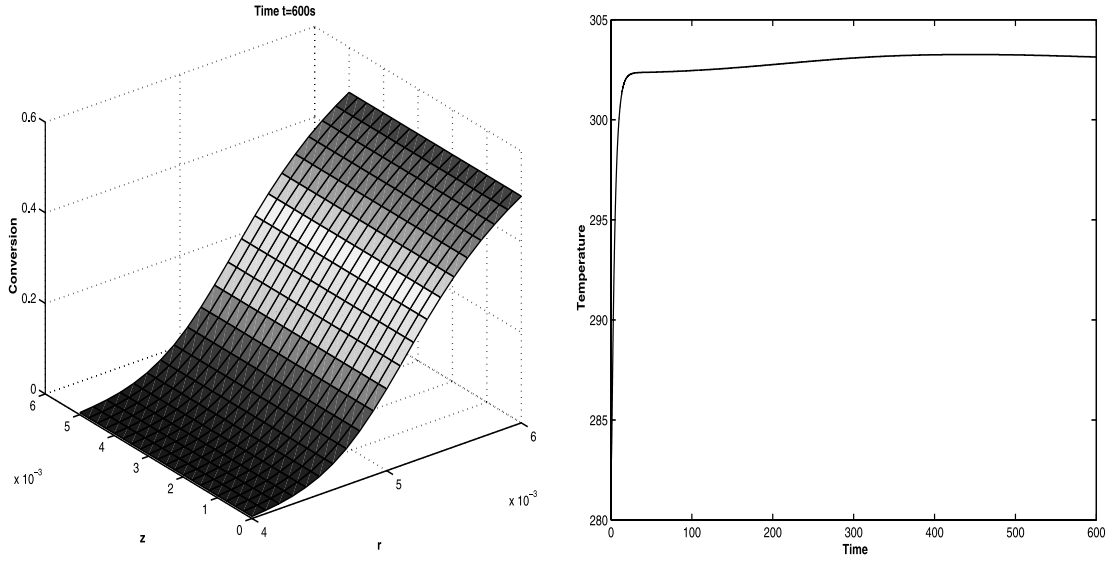

Fig. 4. Thermochemical characteristics of the first sample (spacial distribution of conversion and temperature evolution in the middle point of the sample).

Mohan & Grentzer, 1995; Kinsey, Haji-Sheikh, & Lou, 1997; Nzihou et al., 1999):

$$f^0 = r\rho_{\text{cem}} H^r_{\text{tot}}(x, z, t, T)\frac{\mathrm{d}G}{\mathrm{d}t}, \tag{2.4}$$

where H^r_{tot} is the total heat of reaction of the thermoset.

In the general case, the coupling between two parts of our model, (2.1) and (2.3), is amplified by the dependency of coefficients of Eq. (2.3) on the kinetic reaction. For example, the specific heat can be well approximated by the following formula (Pitchumani & Yao, 1993):

$$C_{\text{p}} \equiv C_{\text{p}}(G, T) = C^1_{\text{p}} G + C^2_{\text{p}}(1 - G), \tag{2.5}$$

where coefficients C^1_{p} and C^2_{p} may be temperature-dependent. In particular, for the acrylic resins these coefficients can be well approximated by the following relationships (the data in Eq. (2.6) were obtained with linear approximations from Fig. 10 in Nzihou et al., 1999):

Table 1
Data for computational experiments performed for acrylic resins

Parameter	Value
ρ_{cem} (kg m^{-3})	1100
k_{cem} (W mK^{-1})	0.17
K_0 (s^{-1})	4.76×10^9
ε_{A} (J mol^{-1})	71.41×10^3
R (J mol^{-1} K^{-1})	8.314472
H^r_{tot} (J g^{-1})	152
r_{12} (m)	2×10^{-3}
r_{22} (m)	5×10^{-3}
$r_{11} = r_{21}$ (m)	4×10^{-3}
k_{b} (W mK^{-1})	0.43
k_{ps} (W mK^{-1})	10.3
$h_1 = h_2$ (m)	5×10^{-3}

$$\begin{aligned} C^1_{\text{p}} &= 629.10 + 3.30T, \\ C^2_{\text{p}} &= -6650.00 + 22.47T. \end{aligned} \tag{2.6}$$

In this case these coefficients can be interpreted as the sum of two terms accounting for contributions before and after polymerisation.

The model is supplemented by initial and boundary conditions and we describe our algorithm for general forms of such conditions in the next section. As a final remark of this section we refer to Table 1 for all data used in our computational experiments reported in Section 4.

3. Numerical algorithm for coupled problems of heat transfer and chemical kinetics in processing polymeric materials

For the solutions of the coupled problems (2.1) and (2.3), we apply an algorithm based on the alternating-triangular methodology which has a number of advantages compared to the techniques proposed earlier for similar types of models, e.g. the ADI method (Kinsey et al., 1997). Consider a general type of nonlinear partial differential equation to which model (2.3) belongs to

$$\begin{aligned} &a^0(x, t, T)\frac{\partial T}{\partial t} \\ &= \sum_{i=1}^{2} \frac{\partial}{\partial x_i}\left[k_i(x, t, T)\frac{\partial T}{\partial x_i}\right] - q^0(x, t, T)T \\ &\quad + f^0(x, t, T), \end{aligned} \tag{3.1}$$

where a^0, q^0, f^0, and k_i, $i = 1, 2$, are given as functions of x, t, and T. Although we have $x_1 = r$ and $x_2 = z$ for our

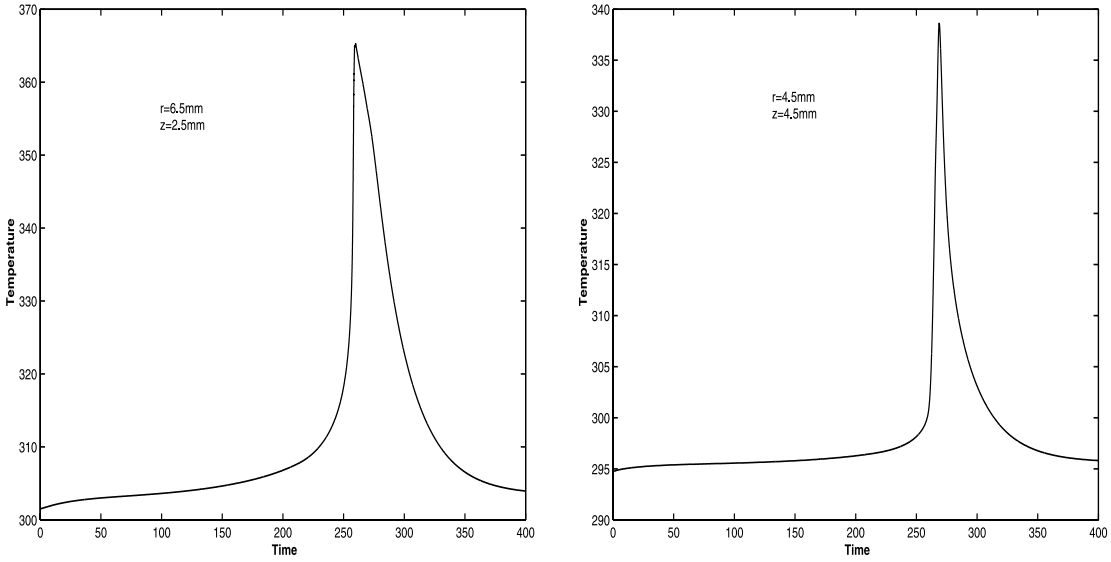

Fig. 5. Temperature evolution in the second sample.

model discussed in Section 2, we use here the indexed spatial coordinates x_i, $i=1, 2$, to simplify notation in the discussion that follows. Again, without lost of generality and to simplify the discussion we consider the spatial region of interest as $G=\{x=(x_1, x_2)\colon 0\le x_i\le L_i\}$ with given L_i, $i=1, 2$. Eq. (3.1) is supplemented by the initial

$$T(x_1, x_2, 0)=T_0(x_1, x_2) \tag{3.2}$$

and boundary conditions

$$\lambda_i^{(1)}\frac{\partial T}{\partial x_i}=\kappa_i^{(1)}(x_j, t, T)T-g_i^{(1)}(x_j, t, T), \quad x_i=0, \tag{3.3}$$

$$-\lambda_i^{(2)}\frac{\partial T}{\partial x_i}=\kappa_i^{(2)}(x_j, t, T)T-g_i^{(2)}(x_j, t, T), \quad x_i=L_i, \quad i=1,2, \quad j=3-i. \tag{3.4}$$

In Eqs. (3.3) and (3.4), values of $\lambda_i^{(1)}$ and $\lambda_i^{(2)}$ are equal to 1 if on the corresponding boundaries of the spatial region G the Neumann are given, or the third-kind boundary conditions. They equal to zero for the Dirichlet boundary conditions. The coefficients in Eqs. (3.1), (3.2), (3.3) and (3.4) satisfy the following conditions

$$\kappa_i^1(x_j, t, T)\ge 0, \qquad \kappa_i^2(x_j, t, T)\ge 0,$$
$$0<c'\le k_i(x, t, T)\le c'', \qquad q^0(x, t, T)\ge 0, \tag{3.5}$$

which include the possibility of fast changing coefficients. Problems with such coefficients arise naturally in many problems pertinent to chemical engineering applications (e.g. Goncharenko & Lychman, 1994; Morton, 1996), and in our case we have to be able to deal with rapid changes in the right hand side part of Eq. (2.3). Such problems with rapidly changing coefficients present serious mathematical difficulties and the development of effective numerical methodologies is required for their treatment. Our computational code for the solution of Eqs. (3.1) and (2.3) is based on the idea of the integro-interpolational approach (Samarskii, 2001). We cover the computational domain with a non-uniform grid, $\hat{\omega}_h$, and consider an elementary space-time cell, $\Delta_{\rm st}$, with $\Delta_{\rm s}=\{(x_1, x_2)\colon x_{1,i_1-0.5}\le x_1\le x_{1,i_1+0.5}, x_{2,i_2-0.5}\le x_2\le x_{2,i_2+0.5}\}$ and $\Delta_{\rm t}=\{t_k\le t\le t_k+\tau\}$. We integrate differential equation (3.1) over the cell $\Delta_{\rm st}$ to get

$$\begin{aligned}&\int_{t_k}^{t_k+\tau}\left\{\int_{x_{2,i_2-0.5}}^{x_{2,i_2+0.5}}[\mathscr{F}^{(1)}_{i_1+0.5}(x_2)-\mathscr{F}^{(1)}_{i_1-0.5}(x_2)]\,{\rm d}x_2\,{\rm d}t\right.\\&\quad\left.+\int_{x_{1,i_1-0.5}}^{x_{1,i_1+0.5}}[\mathscr{F}^{(2)}_{i_2+0.5}(x_1)-\mathscr{F}^{(2)}_{i_2-0.5}(x_1)]\,{\rm d}x_1\,{\rm d}t\right\}\\&\quad-\int_{\Delta_{\rm st}}q^0(x, t, T)T\,{\rm d}x\,{\rm d}t\\&=\int_{\Delta_{\rm st}}a^0(x, t, T)\frac{\partial T}{\partial t}\,{\rm d}x\,{\rm d}t\\&\quad-\int_{\Delta_{\rm st}}f^0(x, t, T)\,{\rm d}x\,{\rm d}t,\end{aligned} \tag{3.6}$$

where ${\rm d}x\equiv{\rm d}x_1{\rm d}x_2$, $\mathscr{F}^{(1)}_{i_1\pm0.5}(x_2)=\mathscr{F}^{(1)}(x_{1,i_1\pm0.5}, x_2)$, and $\mathscr{F}^{(2)}_{i_2\pm0.5}(x_1)=\mathscr{F}^{(2)}(x_1, x_{i_2\pm0.5})$ with $\mathscr{F}^{(i)}(x, t, T)$ being the flux in the direction of x_i, that is

$$\mathscr{F}^{(i)}(x, t, T)=k_i(x, t, T)\frac{\partial T}{\partial x_i}. \tag{3.7}$$

It is also straightforward to get

$$T(x_{1,i_1+1}, x_2, t)-T(x_{1,i_1}, x_2, t)=\int_{x_{1,i_1}}^{x_{1,i_1+1}}\frac{\mathscr{F}^{(1)}(x, t, T)}{k_1(x, t, T)}\,{\rm d}x_1, \tag{3.8}$$

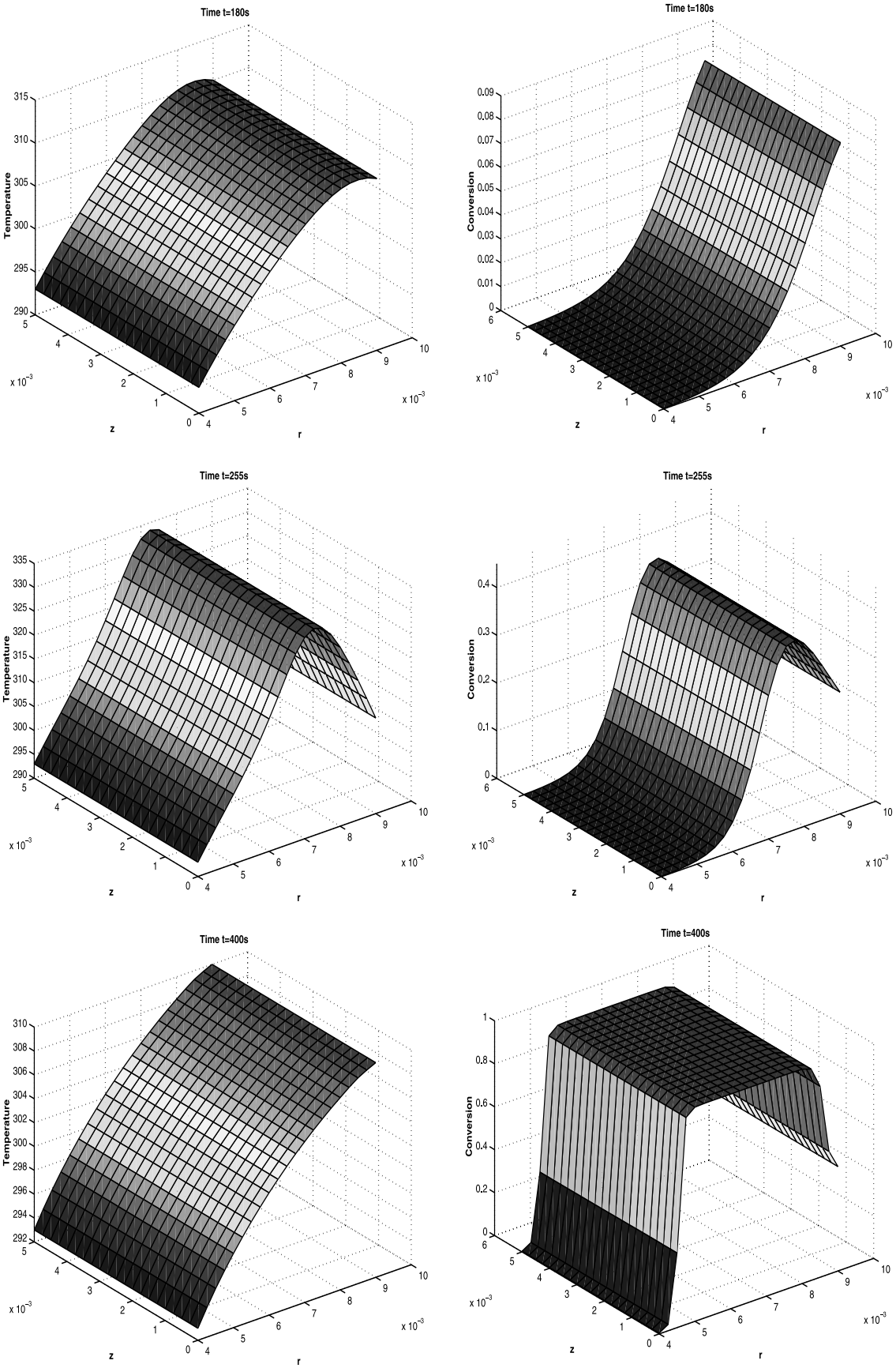

Fig. 6. Spacial distributions of conversion and temperature for different moments of time.

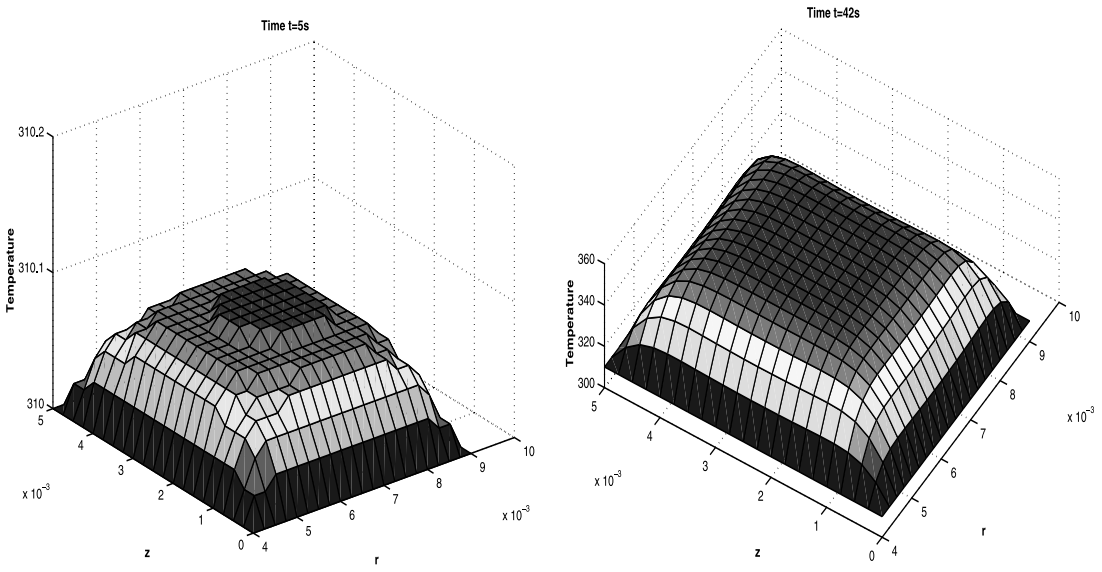

Fig. 7. Spacial temperature distribution in the boundary control and heat pulse simulations.

and a similar expression for $T(x_1, x_{2,i_2+1}, t) - T(x_1, x_{2,i_2}, t)$. By using interpolation formula $\mathscr{F}^{(1)}(x,t,T) \approx \mathscr{F}^{(1)}_{i_1+0.5}(x_2,t,T)$, where $x_1 \in [x_{1,i_1}, x_{1,i_1+1}]$ we come to the following result:

$$T(x_{1,i_1+1}, x_2, t) - T(x_{1,i_1}, x_2, t) \approx \mathscr{F}^{(1)}_{i_1+0.5}(x_2,t,T)\int_{x_{1,i_1}}^{x_{1,i_1+1}} \frac{1}{k_1(x,t,T)}\,\mathrm{d}x_1. \tag{3.9}$$

Again, an analogous expression is derived for $T(x_1, x_{2,i_2+1}, t) - T(x_1, x_{2,i_2}, t)$. Then, we express the values of $\mathscr{F}^{(1)}_{i_1\pm0.5}(x_2,t,T)$ (and $\mathscr{F}^{(2)}_{i_2\pm0.5}(x_1,t,T)$) in terms of the solution of the problem and known functions, e.g.

$$\mathscr{F}^{(1)}_{i_1+0.5}(x_2,t,T) \approx T_{x_{1,i_1}}\left[\frac{1}{h^+_{1,i_1}}\int_{x_{1,i_1}}^{x_{1,i_1+1}} \frac{1}{k_1(x,t,T)}\,\mathrm{d}x_1\right]^{-1}. \tag{3.10}$$

The expressions for $\mathscr{F}^{(1)}_{i_1-0.5}(x_2,t,T)$ and $\mathscr{F}^{(2)}_{i_2\pm0.5}$ are obtained in a similar manner. The resulting scheme is *conservative* and for the inner points (i_1, i_2) of the grid in the stationary case this can be represented as follows:

$$\frac{\mathscr{K}^+_1 y_{x_1} - \mathscr{K}_1 y_{\bar{x}_1}}{h_{1,i_1}} + \frac{\mathscr{K}^+_2 y_{x_2} - \mathscr{K}_2 y_{\bar{x}_2}}{h_{2,i_2}} - qy = -f, \tag{3.11}$$

where $y \equiv y(i_1, i_2)$ and by y_{x_i} and y_{x_i} we denoted backward and forward first difference derivatives. The coefficients and the right hand side of Eq. (3.11) are defined as follows:

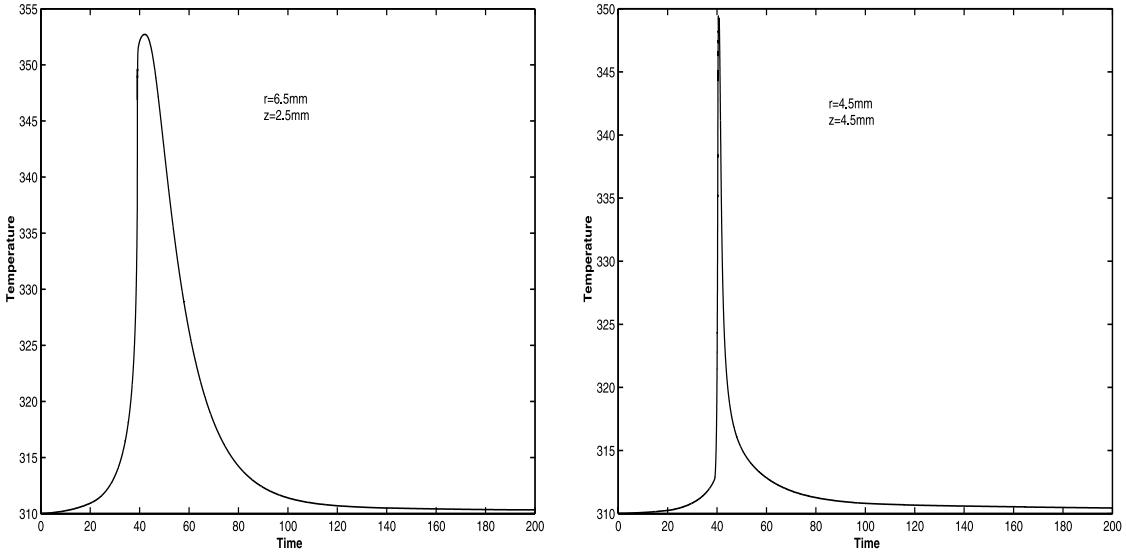

Fig. 8. Temperature evolution in the boundary control and heat pulse simulations.

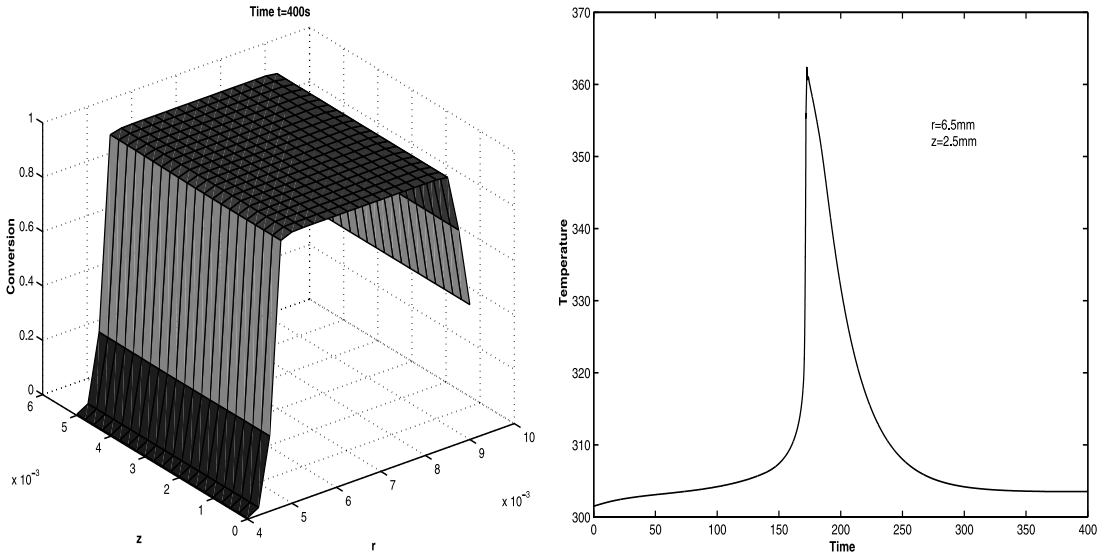

Fig. 9. Spacial distribution of conversion temperature evolution in the heat pulse simulations.

$$q \equiv q(i_1, i_2) = \frac{1}{\hbar_{1,i_1}\hbar_{2,i_2}} \int_{\Delta s} q^0(x)\, \mathrm{d}x,$$
$$f \equiv f(i_1, i_2) = \frac{1}{\hbar_{1,i_1}\hbar_{2,i_2}} \int_{\Delta s} f^0(x)\, \mathrm{d}x, \tag{3.12}$$

$$\mathscr{K}_1 \equiv \mathscr{K}_1(i_1, i_2) = \frac{1}{\hbar_{2,i_2}} \int_{x_{2,i_2-0.5}}^{x_{2,i_2+0.5}} \left[\frac{1}{h^-_{1,i_1}} \int_{x_{1,i_1-1}}^{x_{1,i_1}} \frac{1}{k_1(x)}\, \mathrm{d}x_1 \right]^{-1} \mathrm{d}x_2 \tag{3.13}$$

(with an analogous formula for $\mathscr{K}_2$), $\mathscr{K}_1^+ \equiv \mathscr{K}_1^+(i_1, i_2) = \mathscr{K}_1(i_1 + 1, i_2)$, $\mathscr{K}_2^+ \equiv \mathscr{K}_2^+(i_1, i_2) = \mathscr{K}_2(i_1, i_2 + 1)$. Boundary conditions are approximated by integrating the original differential equation over the cell

$$\Delta_s^{(1)} = \{(x_1, x_2):\quad L_1 - 0.5h^-_{1,N_1} \le x_1 \le L_1,\quad x_{2,i_2-0.5} \le x_2 \le x_{2,i_2+0.5}\}$$

and then using approximate formula (3.10) and computing values of $\mathscr{F}^{(1)}_{N_1}(x_2)$, $\mathscr{F}^{(2)}_{N_2}(x_1)$ from boundary condition (3.4) for $x_i = L_i = x_{i,N_i}$, where $i = 1, 2$. The result is

$$\frac{1}{\hbar_i}(g_i^{(2)} - \kappa_i^{(2)} y - \mathscr{K}_i y_{\bar{x}_i}) + (\mathscr{K}_j y_{\bar{x}_j})_{\hat{x}_j} - qy = -f, \quad x \in \hat{\omega}_j(L_i), \quad i = 1, 2,\ j = 3 - i, \tag{3.14}$$

where $y_{\bar{x}_j \hat{x}_j}$ denotes the second difference derivative constructed on our grid, and other notations are conventional for theory of difference schemes (e.g. Samarskii, 2001). For the grid prototypes of functions $\kappa_i^{(2)}$ and $g_i^{(2)}$ in Eq. (3.4) we used the same notation.

For the solution of obtained discretised system we implemented an effective alternating-triangular methodology with ordered Chebyshev set of iterative parameters. In particular, the constructed discrete scheme can be written in the following generic form:

$$\Lambda y \equiv \sum_{i=1}^{2} \Lambda_i y = -\varphi, \qquad x \in \hat{\omega}_h, \tag{3.15}$$

where $\varphi = f + \varphi_1 + \varphi_2$ and $x \in \hat{\omega}_h$, and for $i = 1, 2$

$$\Lambda_i y = \begin{cases} \dfrac{2}{h_i^+}\mathscr{K}_i^+ y_{x_i} - \left(\dfrac{2}{h_i^+}\mathscr{K}_i^{(1)} + \dfrac{1}{2}q\right)y, & x_i = 0, \\ (\mathscr{K}_i y_{x_i})_{\hat{x}_i} - \frac{1}{2}qy, & x_i \ne 0, L_i, \\ -\dfrac{2}{h_i^-}\mathscr{K}_i y_{x_i} - \left(\dfrac{2}{h_i^-}\mathscr{K}_i^{(2)} + \dfrac{1}{2}q\right)y, & x_i = L_i,\ \ x_j \in \hat{\omega}_j, \end{cases}$$

$$\varphi_i = \begin{cases} \dfrac{2}{h_i^+}g_i^{(1)}, & x_i = 0, \\ 0, & x_i \ne 0, L_i \\ \dfrac{2}{h_i^-}g_i^{(2)} & x_i = L_i,\ \ x_j \in \hat{\omega}_j, \end{cases}$$

or simply as

$$Ay = \varphi, \tag{3.16}$$

to which we apply an implicit two-layer scheme in the following general form:

$$\frac{B(y_{k+1} - y_k)}{\tau_{k+1}} + Ay_k = \varphi, \quad k = 0, 1, 2, \ldots \tag{3.17}$$

Parameters $\{\tau_{k+1}\}$ should be chosen in some optimal way, whereas B has to be constructed as a product of easily invertible operators. In this paper we use the alternating-triangular method with the optimal Chebyshev choice of parameters (Samarskii, 2001). We choose

the operator B in the form

$$B=(D+\omega_0 A_1)D^{-1}(D+\omega_0 A_2),\quad \omega_0>0, \tag{3.18}$$

where

$$Dy=\mathrm{d}(x)y,\qquad \mathrm{d}(x)>0,\qquad x\in\hat{\omega}_h,$$
$$A=A_1+A_2,\qquad A_1^*=A_2. \tag{3.19}$$

We assume that inequalities

$$\delta D\le A,\qquad A_1D^{-1}A_2\le\frac{\Delta}{4}A,\qquad \delta>0, \tag{3.20}$$

$$\Delta>0$$

are satisfied with certain constants δ and Δ. Then we define parameters τ_{k+1} and ω_0 in the following way:

$$\omega_0=2\sqrt{\delta\Delta},\qquad \tau_k=\frac{\tau_0}{1+\rho_0\sigma_k^*}, \tag{3.21}$$

where

$$\tau_0=\frac{2}{\gamma_1^*+\gamma_2^*},\qquad \gamma_1^*=\frac{\delta}{2(1+\sqrt{\eta})},\qquad \gamma_2^*=\frac{\delta}{4\sqrt{\eta}},$$
$$\rho_0=\frac{1-\psi}{1+\psi},\qquad \psi=\frac{\gamma_1^*}{\gamma_2^*},\qquad \eta=\frac{\delta}{\Delta},$$

and $\sigma_k\in\Sigma_{n_0}^*$, where $k=1,\ldots,n_0$. The set

$$\Sigma_{n_0}^*=\left\{\cos\left(\frac{2i-1}{2n_0}\right)\pi,\quad 1\le i\le n_0\right\} \tag{3.22}$$

is a specially ordered set of the roots of Chebyshev polynomial degree n_0. For more details on the ordering procedure the reader may consult Samarskii (2001). Note that if the error of the alternating-triangular method has to be decreased by the factor of ε it is sufficient to perform n_0 iterations, where $n_0\ge\ln(2/\varepsilon)/(2\sqrt{2}\sqrt[4]{\eta})$. The choice of accelerating parameters δ and Δ is a quite involved task that requires the application of discrete analogues of Green's formulae (for further details on this choice the interested reader may consult Melnik (2000)). The described algorithm, implemented into a software code called ALTPACK, constitutes a major block for the solution of the coupled system of Eqs. (2.1) and (2.3) which we perform in an efficient iterative manner. In particular, taking temperature from the initial condition we solve the kinetic reaction equation and determine $\mathrm{d}G/\mathrm{d}t$ at time $t_1=t_0+\tau$ for all spatial points (note that the kinetic reaction rate is a spatially dependent function). The reaction kinetic equation is solved with a two-step block Runge-Kutta-Fehkberg (RKFC) procedure called kinetics.f that uses interpolation to produce output at "off-step points" efficiently. This is a modified procedure developed originally by J.R. Cash and H.A. Watts (see Netlib Software Library). In the context of our problem, the starting point of computations with this model has to be chosen greater than zero. The result of computation of the conversion rate (stored in the array Y_p) is fed into the right hand side (F_p) in polymer.f (a subroutine in ALTPACK). The value of the conversion rate, $\mathrm{d}G/\mathrm{d}t$, will then serve as the input for the package ALTPACK which solves Eqs. (2.3) and (2.4) and hence determines the temperature at the new time layer.

4. Computational experiments

It is known that the analysis of thick composites is inherently more difficult compared to their thin counterparts, and the development of models for curing such composite parts constitutes an important task in many chemical engineering applications (e.g. White & Kim, 1996). The difficulties stem from the fact that a thermal lag and spiking are much more common phenomena for thick composites compared to thin polymeric composites. We demonstrate this statement by the following example. Consider two samples made of acrylic resins (see Fig. 3). These materials are indispensable in many applications ranging from automotive industry (Petit et al., 2001) to biomedical applications (Lewis, 1996; Halvorson, Erickson, & Davidson, 2002). As evident from Table 1, the thickness of the first sample is only 2 mm while the second sample has thickness of 5 mm. The developed software code described in Section 3 is capable of dealing with both of these situations with a complete range of initial and boundary conditions encountered in practical applications. In what follows we describe three groups of computational experiments. In the first group, we consider the Dirichlet boundary condition at side AD: $T=T_{AD}$. The interpretation of the considered situation can be analogous to that considered previously by Nzihou et al. (1998, 1999) where the prosthesis (index "ps" in our notation) is fixed to a bone (index "b" in our notation) by the layer of bone cement (acrylic resin), which is the polymeric material of interest. In this case we can approximate the boundary condition at the BC side by the following boundary conditions of third kind $-\partial T/\partial r=C(T-T_b)$ with C taken in our experiments as $C=k_b/(5\times10^{-3}k_p)$. In the first set of experiments we impose the Neumann boundary conditions at boundaries AB and CD: $\partial T/\partial z=0$. The initial boundary conditions are chosen in the form

$$T=ar+c \text{ for } t=t_0 \text{ with } a=(T_b-T_{ps})/\Delta r \text{ and } c$$
$$=T_b-(T_b-T_{ps})r_2/\Delta r, \tag{4.1}$$

where $\Delta r=r_2-r_1$. The initial temperatures of prosthesis (T_{pros}) and bone (T_b) are assumed to be at 293 and 310 K, respectively. We solve the coupled heat transfer/reaction kinetics problem for these two geometries. For the first sample, the spatial distribution of conversion at

time moment $t = 600$ s is shown in Fig. 4 (left). On the right (the same Fig. 4) we present the temperature evolution at the middle point of the structure. It is seen that the conversion is nonuniform along the r-direction and its evolution leads to an increase in temperature which stabilises at around 303 K. The evolution is fundamentally different for thick composites. The same conditions were applied to the analysis of the second sample presented in Fig. 3. The result is drastically different clearly demonstrating that the heat produced as a result of the reaction is trapped inside of the structure. Moreover, after 260 s of the process of curing, a spike in the temperature profile can be observe not only in the middle of the structure (see Fig. 5 (right)), but also closer to its boundary (see Fig. 5 (left)), although with a smaller magnitude due to the Neumann boundary conditions imposed. The evolution of temperature and conversion for the second sample are shown in Fig. 6. The initially linear-in-r profile of temperature and almost zero degree of conversion (taken at 10^{-5}) evolves, as expected, with a pronounced increase in temperature propagating from the higher temperature end of the structure. There are two competing requirements in this coupled process, namely maximising the degree of curing and minimising the peak of temperature. As a result of this competition, conversion evolves to a typical (for these boundary conditions) spatial pattern presented in Fig. 6 (the bottom right), while temperature profile becomes close to linear again. The dynamics of peak temperature propagation (see, for example, Fig. 5) is intrinsically coupled with the evolution of the degree of conversion. As a result, we can attempt to control the onset of the thermal spiking phenomenon by exposing the sample to some additional heating pulse, e.g. by laser irradiation and/or by the boundary control. In particular, the technique known as stereolithography is based on curing polymers by exposing their small zones to laser irradiation (e.g. Maffezzoli & Terzi, 1998). In our second group of experiments we impose Dirichlet boundary conditions at 310 K and expose our second sample to a small concentrated heat pulse. Two snapshots of temperature evolution are presented in this case, for times 5 and 42 s, in Fig. 7. In this case, the onset of thermal spiking in the sample happens much quicker compared to what we have observed in the first group of computational experiments. As demonstrated in Fig. 8, after 40 s of evolution the spiking phenomenon is observed. In our final group of computational experiments we return to our original boundary conditions discussed at the beginning of this section. In this case, due to the Neumann boundary conditions imposed, the onset of thermal spiking phenomenon slows down compared to the second group of computational experiments. In Fig. 9 we present the degree of conversion and temperature evolution for this case. Note finally that compared to the first group of computational experiments the onset of thermal spiking is observed at an earlier stage due to the heat pulse applied.

5. Concluding remarks

In this paper the problem of coupled kinetics and heat transfer has been solved with an efficient numerical algorithm based on the alternating-triangular methodology. We have focused on the problem that consists of a phenomenological kinetic model coupled to an energy balance model. The algorithm proposed for the solution of this problem allows one to determine simultaneously the fractional conversion, the conversion rate, and the temperature profile.

The coupling between kinetics and heat transfer is especially important in analysing spiking and thermal lag phenomena in polymeric materials. With the algorithm developed we have analysed numerically the onset of thermal spiking phenomena in polymeric (acrylic) resins. Results of numerical predictions have been discussed in detail. From a numerical point of view, the algorithm is more efficient compared to alternating-direction implicit methodologies of the Peaceman-Rachford-type traditionally applied to similar problems.

Acknowledgements

Fruitful discussions with Drs. F. de Hoog, D. Jenkins, and J. Hodgkin of CSIRO on the topics of this work are gratefully acknowledged.

References

Adolf, D. B., et al. (1998). Stresses during thermoset cure. *Journal of Materials Research 13*, 530–550.

Buckmaster, J., & Vedarajan, T. G. (1997). Self-heating effects in thermoset composites. *Journal of Composite Materials 31*, 2–20.

Covas, J. A. (1994). The inverse problem in polymer processing. In J. A. Covas, et al. (Eds.), *Rheological fundamentals of polymer processing* (pp. 385–406). Dordrecht: Kluwer Academic Publishers.

Cristini, V., Macosko, C. W., & Jansseune, T. (2002). A note on transient stress calculation via numerical simulations. *Journal of Non-Newtonian Fluid Mechanics 105*, 177–187.

Ding, Z. M., et al. (2000). Numerical and experimental analysis of resin flow and cure in RIP. *Polymer Composites 21* (5), 762–778.

Flipsen, T. A. C., et al. (1996). A novel thermoset polymer optical fiber. *Advanced Materials 8*, 45–48.

Goncharenko, V. M., & Lychman, V. V. (1994). Numerical solution of a boundary-value problem. *Journal of Mathematical Sciences 72*, 3116–3119.

Halvorson, R. H., Erickson, R. L., & Davidson, C. L. (2002). Energy dependent polymerization of resin-based composite. *Dental Materials 18*, 463–469.

Kim, C., et al. (1995). The continuous curing process for thermoset polymer composites. *Journal of Composite Materials 29*, 1222–1253.

Kinsey, S. P., Haji-Sheikh, A., & Lou, D. Y. S. (1997). A thermal model for cure of thermoset composites. *Journal of Materials Processing Technology 63*, 442–449.

Lewis, G. (1996). Bioengineering science news: research directions in acrylic bone cement studies. *Biomedical Engineering Society Bulletin 20* (1), 3–11.

Li, W., & Lee, L. J. (1998). Shrinkage control of low-profile unsaturated polyester resins cured at low temperature. *Polymer 39*, 5677–5687.

Li, L., Sun, X. D., & Lee, L. J. (1999). Low temperature cure of vinyl ester resins. *Polymer Engineering and Science 39* (4), 646–661.

Maffezzoli, A., & Terzi, R. (1998). Effect of irradiation intensity on the isothermal photopolymerization kinetics of acrylic resins for stereolithography. *Thermochimica Acta 321*, 111–121.

Melnik, R. V. N. (2000). The alternating-triangular algorithm for the analysis of blow-up and quenching phenomena in nonlinear PDEs. *International Journal of Mathematical Algorithms 2*, 89–120.

Melnik, R. V. N., Uhlherr, A., Hodgkin, J., & de Hoog, F. (2003). Distance geometry algorithms in molecular modelling of polymer and composite systems. *Computers and Mathematics with Applications 45* (1–3), 515–534.

Mohan, R., & Grentzer, T. H. (1995). Process simulation in thermoset composites for cure response and stress prediction. *Journal of Reinforced Plastics and Composites 14*, 72–84.

Morton, K. W. (1996). *Numerical solution of convection-diffusion problems*. London: Chapman & Hall.

Nzihou, A., et al. (1998). A rheological, thermal and mechanical study of bone cement—from a suspension to a solid biomaterial. *Powder Technology 99*, 60–69.

Nzihou, A., Sharock, P., & Ricard, A. (1999). Reaction kinetics and heat transfer studies in thermoset resins. *Chemical Engineering Journal 72*, 53–61.

Petit, H., et al. (2001). Ambient cure high solids acrylic resins for automotive refinish clear coat applications. *Progress in Organic Coatings 43*, 41–49.

Pitchumani, R., & Yao, S.-C. (1993). Non-dimensional analysis of an idealized thermoset composites manufacture. *Journal of Composite Materials 27*, 613–636.

Samarskii, A. A. (2001). *The theory of difference schemes*. New York: Marcel Dekker.

Tokarski, J. S., et al. (1997). Molecular modelling of polymers. *Computational and Theoretical Polymer Science 7*, 199–214.

Torre, L., Maffezzoli, A., & Nicolais, L. (1995). Process modelling of thermoset based composites. *Revue de L'Institut Francais Petrol 50*, 135–139.

White, S. R., & Kim, Y. K. (1996). Staged curing of composite materials. *Composites A 27A*, 219–227.